ELSEVIER

International Journal of Solids and Structures 41 (2004) 5595–5610

INTERNATIONAL JOURNAL OF SOLIDS and STRUCTURES

www.elsevier.com/locate/ijsolstr

The influence of a weld-induced axi-symmetric imperfection on the buckling of a medium-length silo under wind loading

Martin Pircher *

Centre for Construction Technology and Research, Kingswood Campus, Bldg X, University of Western Sydney, Locked Bag 1797, Penrith South DC, NSW 1797, Australia

Received 7 January 2004; received in revised form 1 May 2004
Available online 11 June 2004

Abstract

For particular geometrical constellations of thin-walled cylindrical structures under wind-loading, a peculiar stability failure mode has been observed. This failure mode is characterised by the occurrence of multiple horizontal ripple-like buckles in an area around the upper half of the windward meridian. A recent case study of a cylinder undergoing this type of buckling revealed the strong influence of localised axi-symmetric imperfections on this particular buckling behaviour. For the present paper a detailed investigation into the nature of this influence of such imperfections on the buckling behaviour under wind loading has been performed using finite elements models. A cylinder with a geometry that displayed the particular buckling pattern in question was considered for this study. The parameters describing the nature of the axi-symmetric weld imperfection were varied and their influence on the buckling of these cylinders was studied in detail. The present study draws from insights gained from similar studies for cylinders under axial loading. Many similarities between the two loading cases can be observed and the influence of weld-induced imperfections on the buckling under the two loading types were compared for this paper.

Keywords: Silo; Wind loading; Thin-walled cylinder; Shell structure; Stability; Axi-symmetric imperfection; Weld imperfection

1. Introduction

For cylinders with certain geometrical proportions, a buckling mode under wind loading exists which has not been extensively researched in the past. This buckling mode occurs for cylinders with radius-to-thickness ratios (R_0/t-ratios) and length-to-radius ratios (L/R_0-ratios) typically found for example in tall silos and is characterised by multiple ripple-like buckles in the area around the upper half of the windward meridian (termed the "front" of the cylinder in this paper). A recent case study for a cylinder displaying this type of buckling behaviour (Pircher, 2004) brought attention to the fact that this buckling mode is quite sensitive to the presence of axi-symmetric imperfections. In welded silos and tanks such imperfections are

* Tel.: +61-2-47-360-307; fax: +61-2-47-360-833.
E-mail address: m.pircher@uws.edu.au (M. Pircher).

0020-7683/$ - see front matter © 2004 Elsevier Ltd. All rights reserved.
doi:10.1016/j.ijsolstr.2004.05.001

frequently present due to the building techniques employed for the erection of such structures. Steel plates are typically bent into the required radius and then welded together horizontally and vertically to form the final structure. The horizontal welds commonly span around the whole circumference of these silos and inward-facing geometrical imperfections are typically found around these circumferential welds. The geometry and other properties of these weld-induced circumferential imperfections have been discussed in Pircher et al. (2000). The detrimental influence of axi-symmetric weld-induced imperfections on the buckling behaviour of thin-walled cylinders under axial loading has been well documented in a number of research papers (e.g., Steinhardt and Schulz, 1970; Rotter and Teng, 1989; Pircher and Bridge, 2001). Greiner and Derler (1995) investigated the influence of a number of different imperfection shapes on the buckling of silos under wind loading. However, axi-symmetric welds were not included in their study.

Depending on the geometry of a cylindrical structure three different stability failure modes can be observed (Fig. 1). In low cylinders radial compression at the front of the cylinder causes tangential compressive membrane forces N_φ which result in a buckling mode similar to cylinders under radial compression (mode 1 in Fig. 1). Very long cylinders display a distinctly different failure mode, whereby the compressive axial forces N_x at the back of the cylinder trigger buckling in the lower third of the structure (mode 3 in Fig. 1) (e.g., Schneider and Zahlten, 2004). Mode 2 in Fig. 1 occurs for cylinders within a small range of geometric parameters and is characterised by a number of ripple-like circumferential buckles in the upper half of the meridian facing into the wind. The term "medium-length cylinders" in the context of this papers refers to cylinders displaying this particular buckling mode under wind-loading. This mode was first mentioned by Feder (1975) who reported on the failure of small PVC-specimens in a wind tunnel test with additional axial loading. Greiner and Derler (1995) presented results of a numerical investigation of cylinders under wind loading, some of which also displayed this failure characteristic. In this paper the influence of axi-symmetric weld-induced imperfections on the buckling of a thin-walled cylinder displaying this particular failure mode will be studied.

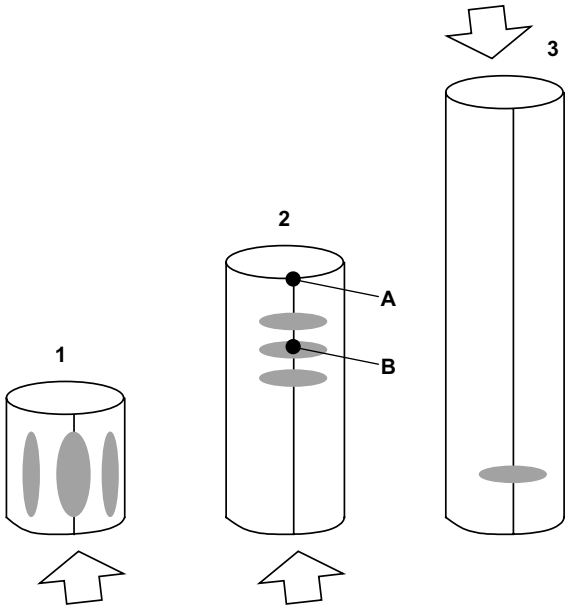

Fig. 1. Buckling of thin-walled cylinders under wind loading.

2. Background

2.1. Structural model

A thin-walled cylindrical shell with fixed bottom support and a diaphragm roof or rigid ring stiffener restricting movement in the tangential and radial direction at the top was modelled using the finite elements method. Fig. 2 captures the geometric properties R_0, L and t of the described structural system and also gives the naming conventions for the membrane stresses σ_x, σ_φ, $\tau_{x\varphi}$ and displacements u, v and w. The geometry of the cylinder analysed for this case study is given by $R_0 = 10$ m, $R_0/t = 400$ and $L/R_0 = 10$. Elastic material properties to resemble the behaviour of steel with a Young's modulus $E = 2.1\text{E}8$ kN/m^2 and a Poisson ratio of $v = 0.3$ were defined. Since buckling was found to take place well in the elastic region of the steel, no material non-linearities were taken into account. The computer model comprised half a cylinder with planes of symmetry along the meridians facing into the wind ($\varphi = 0$) and away from the wind ($\varphi = 180$).

2.2. The failure mode

The particular stability failure mode for medium-length cylinders which is the topic of this paper was first mentioned in Feder (1975) and then again in Greiner and Derler (1995). A detailed case study of the failure of a medium-length thin-walled cylinder under wind loading displaying this failure mode is given in Pircher (2004). A cylinder with the same geometry as in this case study will be used for this paper. The displaced shapes of a cylinder with no imperfections and with the same geometry as studied in this paper is shown in Fig. 3 for various points along the load–displacement path under wind loading. A snap-through failure mode into one large buckle covering a large area on the front side of the cylinder (long axial wavelength mode) occurs first, closely followed by bifurcation into a failure mode with multiple horizontal ripple-like buckles around two-thirds height of the cylinder (short axial wavelength mode). Two effects have been found to contribute to the particular buckling behaviour of such cylinders: first, the presence of axial compressive stresses in the upper half of the front-side of the cylinder and secondly, ovalisation of the

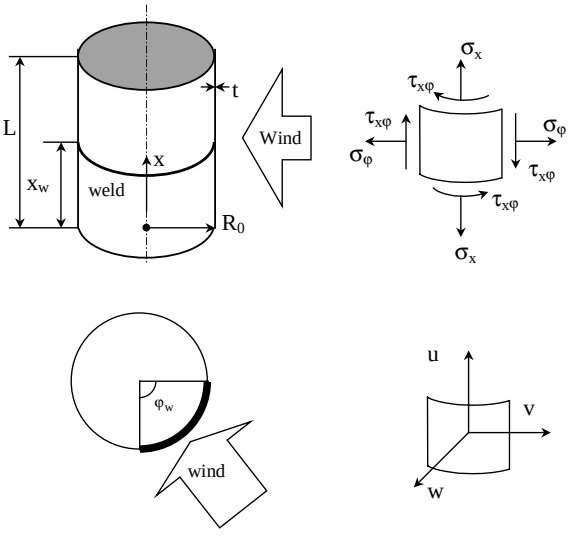

Fig. 2. Structural system, membrane stresses and displacements.

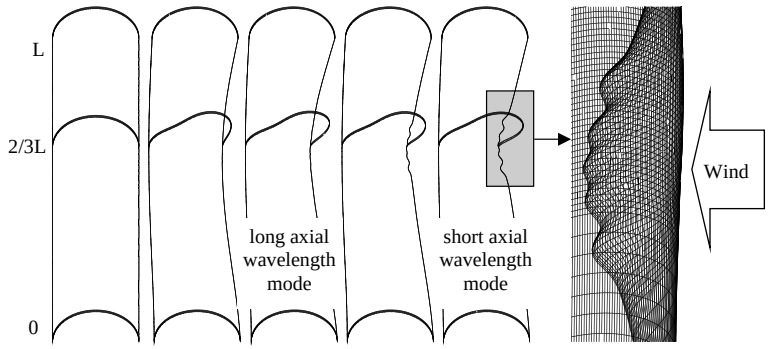

Fig. 3. Displaced shapes of the cylinder under wind loading at selected points along the load–displacement path.

cross-section of the cylinder in areas away from the bottom and top supports. It was shown in Pircher (2004) that the compressive axial forces trigger buckling which is aided by the decreased local resistance of the cylinder due to the ovalised cross-section in this area. A supplementary eigenmode analysis found two closely spaced bifurcation points which account for this buckling behaviour. Geometrically non-linear effects contribute greatly to the buckling behaviour with a linear buckling analysis predicting an entirely different failure mode. A brief imperfection sensitivity study in Pircher (2004) showed that for many different imperfection shapes the structure was found to transform straight into the short axial wavelength mode without experiencing snap-through buckling into the long axial wavelength mode first.

2.3. Wind loading

A thorough discussion of many of the factors involved in wind pressure on circular cylindrical structures can be found in Esslinger (1971), Kwok (1985) and Macdonald et al. (1988). The radial wind pressure varies around the circumference and up the height of the cylinder. For this paper the governing radial component of the wind loading around the circumference was assumed to be given by

$$p_{\mathrm{Wind}}(\varphi) = \sum_{m=1}^{n} p_m \cos(m\varphi) = p_r \sum_{m=1}^{n} c_m \cos(m\varphi), \tag{1}$$

where p_r is the actual wind pressure onto the meridian facing the wind, c_m are the amplitudes of the Fourier waves, m is the number of the individual Fourier waves and $p_{\mathrm{Wind}}(\varphi)$ is the resulting wind load. The material developed for this paper uses values for c_m which have been suggested by Greiner and Derler (1995) with $c_0 = -0.65$, $c_1 = 0.37$, $c_2 = 0.84$, $c_3 = 0.54$, $c_4 = -0.03$ and $c_5 = -0.07$. Wind pressure up the height of the cylinder was assumed to be constant and the roof was not loaded. This structural system and model for wind loading has been used in the past for investigations of thin-walled cylinders under wind loading (e.g., Greiner, 1983; Pircher et al., 2001b). For this paper all critical loads for imperfect structures $p_{\mathrm{cr,imp}}$ are given in relation to the maximum load of the perfect structure which was found to be $p_{\mathrm{cr,perfect}} = 5.83\ \mathrm{kN/m^2}$. A comparison of the stresses present at buckling under wind loading with the critical stresses for pure axial and radial loading must take the significant ovalisation due to wind loading into account (Fig. 6). This comparison along with a detailed explanation of the buckling mechanism of the geometrically perfect system has been published in Pircher (2004). At this point it should be remarked that the displacements of the loaded structure also have an influence on the wind loading pattern of the structure. This effect was not taken into account for this investigation.

2.4. The axi-symmetric weld imperfection

Axisymetric imperfections in circular cylindrical steel shell structures such as silos or tanks occur during construction when rolled steel plates are formed into a series of individual strakes and joined together by circumferential welds. The cooling of the welding material at the circumferential joints causes small inward deflections in the finished structure which are also accompanied by residual stresses. Pircher et al. (2001a) calibrated a theoretical approach based on elastic shell theory (Berry et al., 2000) against measured data and suggested a shape function given by

$$w(x) = A\,\mathrm{e}^{-\pi x/\lambda}\left(\cos\frac{\pi x}{\lambda} + \zeta \sin\frac{\pi x}{\lambda}\right), \tag{2}$$

in which $w(x)$ is the radial deviation from the perfect cylinder and A is the amplitude of the localised imperfection. The parameter ζ defines the degree of roundness directly at the weld and is a measure for the variation of stiffness of the weld material during cooling of the weld. Parameter λ is the half-wavelength of the imperfection in the longitudinal direction which will be related to the linear meridional bending half-wavelength λ_0 of a thin-walled cylinder given by

$$\lambda_0 = \pi\sqrt{\frac{R_0 t}{\sqrt{12(1-\nu^2)}}} \approx 2.444\sqrt{R_0 t}. \tag{3}$$

Other shape functions which have been suggested in the literature can be approximated by the given function by variation of the ζ and λ parameters which is documented in Pircher et al. (2001a). In a number of papers (e.g., Rotter and Teng, 1989; Teng and Rotter, 1992; Pircher and Bridge, 2001; Song et al., 2004), the shape function given in Eq. (2) (or simplifications thereof) was used for an investigation of axi-symmetrically imperfect cylinders under axial loading. The given function will be used again in this paper.

2.5. Imperfection sensitivity

A preliminary parametric study to investigate the imperfection sensitivity of the thin-walled cylinder under wind loading in this particular case study was performed in Pircher (2004). Several types of geometric imperfections were considered, among them eigenmode-affine shapes, a dent and axi-symmetric shapes. Localised axi-symmetric imperfections were found to be by far the most detrimental type of imperfection among the shapes tested in this paper. These results along with the fact that circumferential weld-induced imperfections have been shown to have an important influence on the buckling behaviour of thin-walled cylinders under axial loading led to the research results summarised in the present paper.

3. Results

3.1. Buckling and post-buckling behaviour

The buckling and the initial post-buckling behaviour changes due to the introduction of an axi-symmetric weld-like imperfection. Fig. 4(a) shows the front meridian of a perfect cylinder for selected points on the load–displacement curve for point B (Fig. 1). The load–displacement curve for this cylinder is shown in Fig. 4(b). The buckling behaviour with both stability failure modes as described above is clearly visible. The same diagrams for an axi-symmetric imperfection with $\xi = 0.5$ and $\lambda/\lambda_0 = 2.0$ are shown in Fig. 5(a) and (b). Fig. 6 shows a horizontal cut through the cylinder at buckling for the perfect and the imperfect structure. The structure never displays the long axial wavelength mode but snaps straight into a

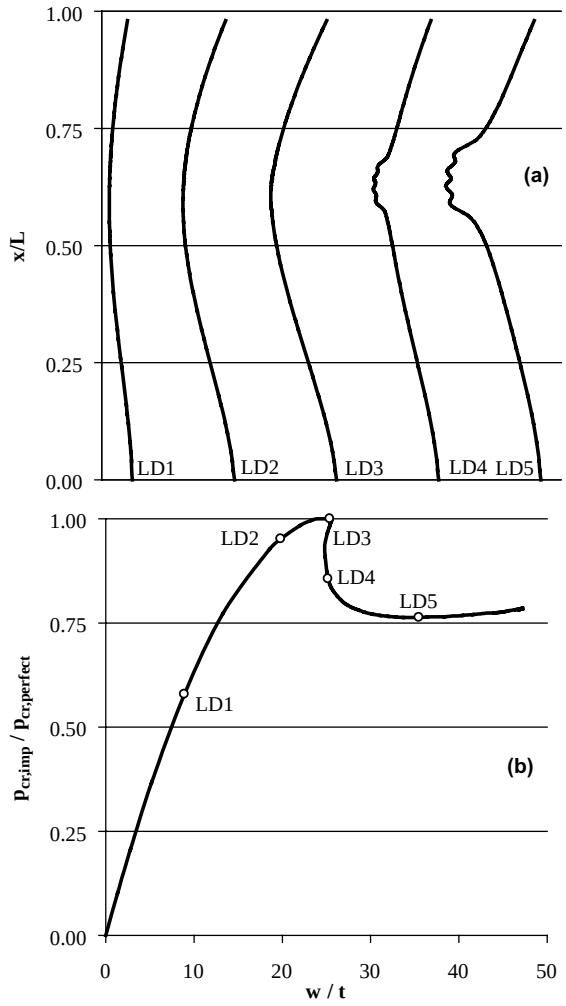

Fig. 4. Geometrically perfect model: front meridian (a) at selected points during load–displacement path (b).

buckling mode which is best characterised as a single horizontal fold-like buckle across the front of the cylinder.

Various load–displacement characteristics (point B) for the same imperfection geometry ($\xi = 0.5$ and $\lambda/\lambda_0 = 2.0$), with various amplitudes ($0 < A/t < 3.0$) are given in Fig. 7. For imperfection amplitudes up to approximately $A/t = 1.2$, a clear local maximum load level can be observed after which the load-bearing capacity drops off steeply before reaching a post-buckling minimum. After this minimum, in the presence of considerable displacements, the wind load can be increased again. The post-buckling minimum is in a similar place for all these load–displacement characteristics.

For cylinders with an axisymmetric imperfection with an amplitude $A/t > 1.2$ no distinct maximum can be defined in the load–displacement characteristics and no distinct point of stability loss could be observed during the analysis. The transition from the "pre-buckling" section of the load–displacement curve into the "post-buckling" section was found to be gradual. The imperfect structures were found to experience increased deflection rates and the load–deflection path merged with the post-buckled load deflection path of

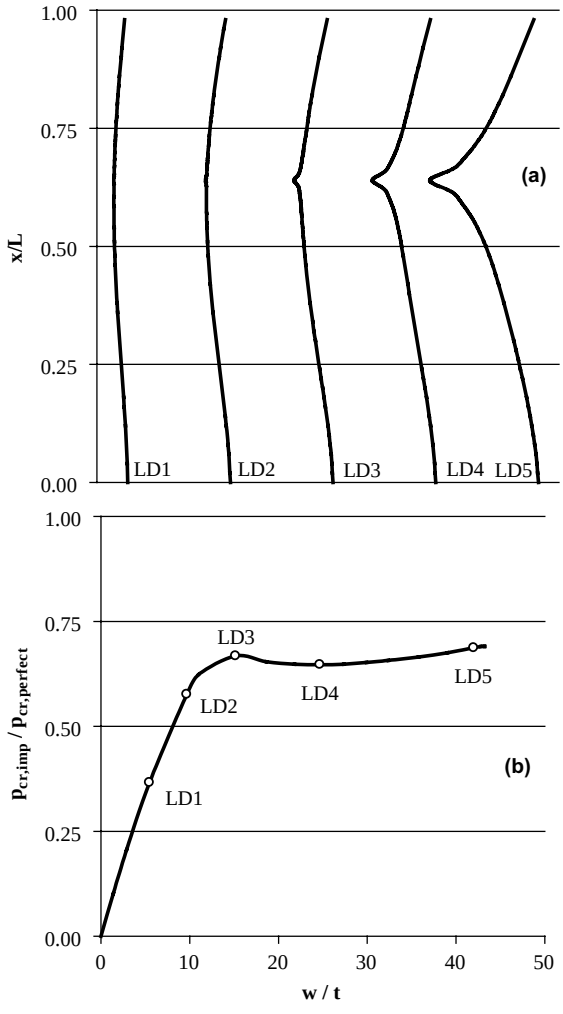

Fig. 5. Imperfect model ($\xi = 0.5,\ \lambda/\lambda_0 = 2.0$): front meridian (a) at selected points during load–displacement path (b).

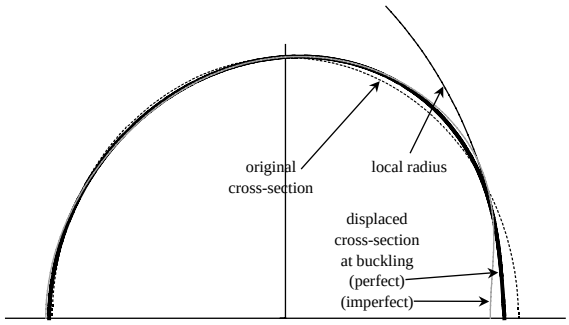

Fig. 6. Horizontal cut at weld height.

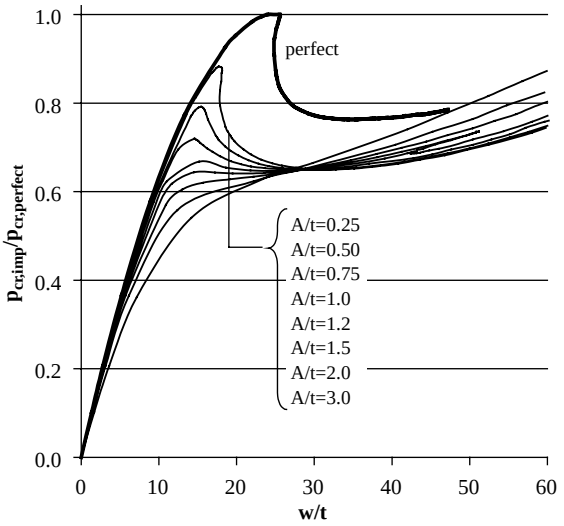

Fig. 7. Influence of axi-symmetric imperfections on the initial post-buckling behaviour.

the structures with smaller imperfection amplitudes $A/t < 1.2$. The load–displacement curves for all imperfect FE models intersected at a point near the post-buckling minimum after which an increase in load was possible beyond the initial maximum point. The displacements at this stage are large and an analysis beyond this stage would have to consider displacement-dependent loading and also dynamic effects in order to simulate wind loading conditions properly.

For the results presented in this paper geometrically non-linear analyses were performed. The critical loads given in the following are local load maxima as explained above. For weld amplitudes $A/t > 1.2$ no such maxima can be defined. Since the typical weld imperfection found in silos usually does not exceed this measure (Steinhardt and Schulz, 1970; Pircher et al., 2001a) it was found sufficient for the purpose of this paper to limit the investigation to amplitudes A/t less or equal 1.2.

3.2. Weld position

In a first series of analyses the influence of the weld position x_w on the buckling resistance was investigated. The shape of the imperfection was set according to Eq. (2) with parameters $\lambda/\lambda_0 = 1.0$ and $\zeta = 0.5$. Fig. 8 illustrates this influence for various amplitudes of the imperfection. All graphs clearly show a minimum of buckling resistance when the weld imperfection is situated at $x_w/L = 0.64$. For all further analyses presented in this paper the axi-symmetric weld-like imperfection was placed at this position in the finite element model.

3.3. Shape of the weld imperfection

Three non-dimensional parameters determine the shape of the axi-symmetric weld imperfection according to Eq. (2): the amplitude A/t, the roundness parameter ζ and the half-wavelength λ/λ_0. FE models with imperfections of five different amplitudes ($A/t = 0.25,\ 0.50,\ 0.75,\ 1.0,\ 1.2$) were built. For each amplitude a diagram giving the buckling strength as a function of the half-wavelength was compiled for three values of the roundness parameter ζ ($\zeta = 0.0,\ 0.5,\ 1.0$). The influence of these three parameters on the buckling resistance is given in the five diagrams presented in Figs. 9–13. As can be seen in these

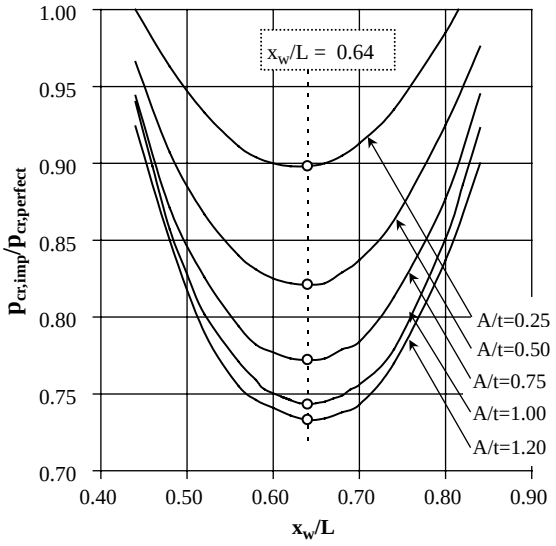

Fig. 8. Effect of weld position on the buckling strength.

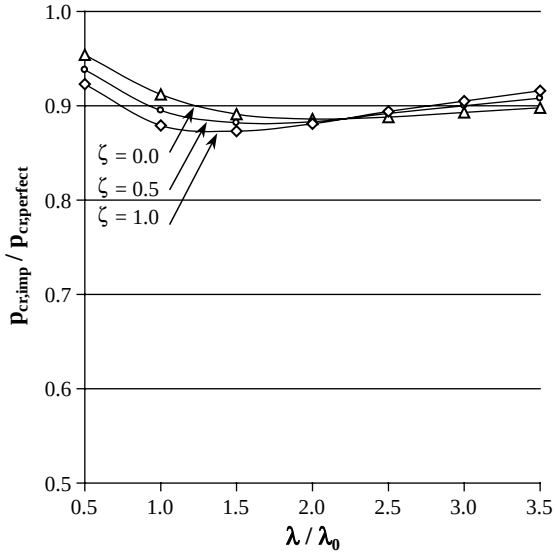

Fig. 9. Influence of the parameters ζ and λ/λ_0 on the buckling resistance for an imperfection amplitude $A/t = 0.25$.

diagrams, all three parameters influence the buckling resistance considerably. All diagrams show an intersection point at λ/λ_i where the graphs for different values of ζ intersect. For values of $\lambda/\lambda_0 < \lambda_i/\lambda_0$ imperfections of $\zeta = 1.0$ yield the lowest results for the buckling resistance, for values of $\lambda/\lambda_0 > \lambda_i/\lambda_0$ welds of $\zeta = 0.0$ yield the lowest results. The position of this intersection point (λ_i/λ_0) and also the position of the minimum of buckling resistance ($\lambda_{\min}/\lambda_0$) varies depending on the amplitude of the imperfection as shown in Fig. 14. The decrease in buckling resistance as a function of the imperfection amplitude is shown in Fig. 15. The decrease in buckling strength under wind loading is considerable. For a weld imperfection with an

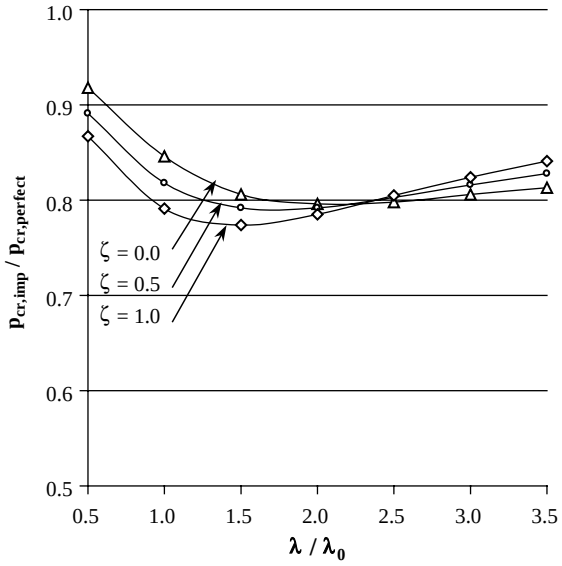

Fig. 10. Influence of the parameters ζ and λ/λ_0 on the buckling resistance for an imperfection amplitude $A/t = 0.50$.

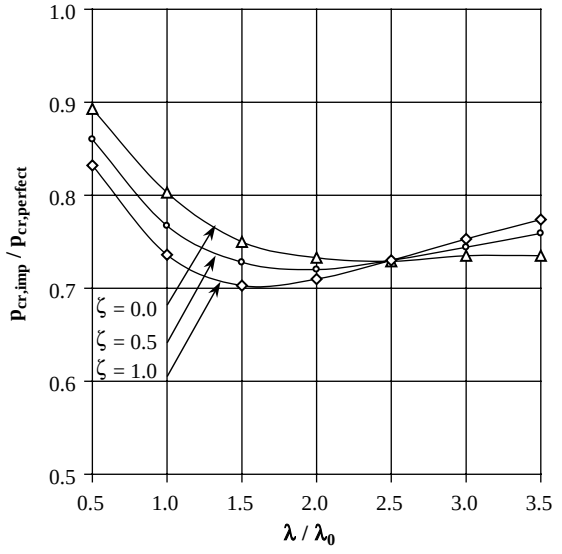

Fig. 11. Influence of the parameters ζ and λ/λ_0 on the buckling resistance for an imperfection amplitude $A/t = 0.75$.

amplitude of $A/t > 1.0$ the buckling resistance is only 65% of the resistance of the nominally perfect cylinder.

3.4. Partial weld

In many cases circumferential welds in existing silos cause imperfections along significant portions of the circumference. Such an imperfection may be more severe in some places than in others. In order to

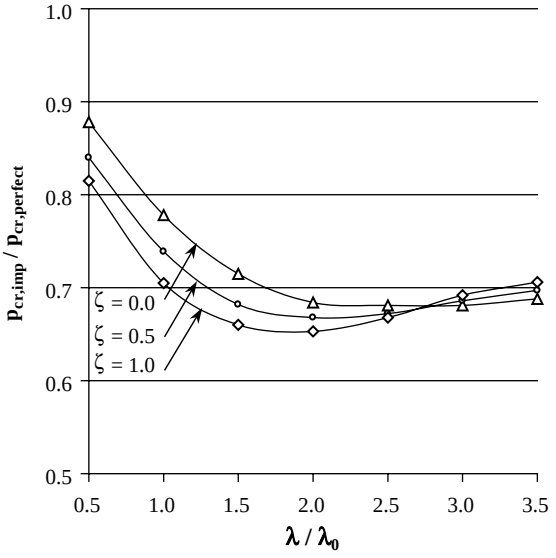

Fig. 12. Influence of the parameters ζ and λ/λ_0 on the buckling resistance for an imperfection amplitude $A/t = 1.0$.

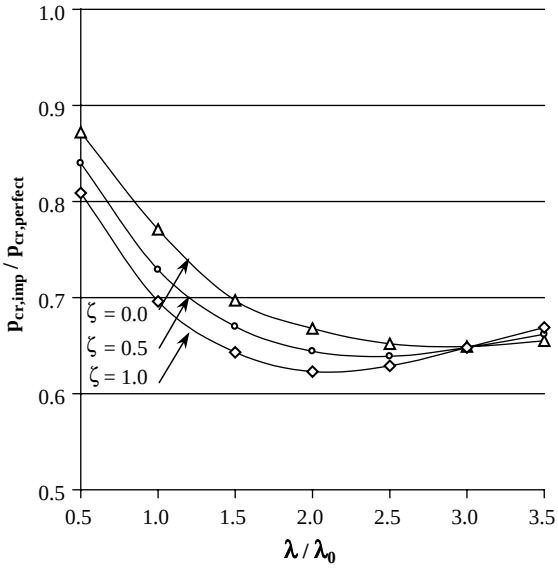

Fig. 13. Influence of the parameters ζ and λ/λ_0 on the buckling resistance for an imperfection amplitude $A/t = 1.2$.

investigate the influence of circumferential imperfections which span only across a part of the circumference (φ_w), a series of analyses with partial weld imperfections was performed. Fig. 16 shows the buckling resistance for partial welds with an amplitude of $A/t = 0.25$ for various shape parameters λ/λ_0 and ζ. A minimum in buckling resistance can be observed at $\varphi_w = 20°$. Shortly after this minimum the graph for the

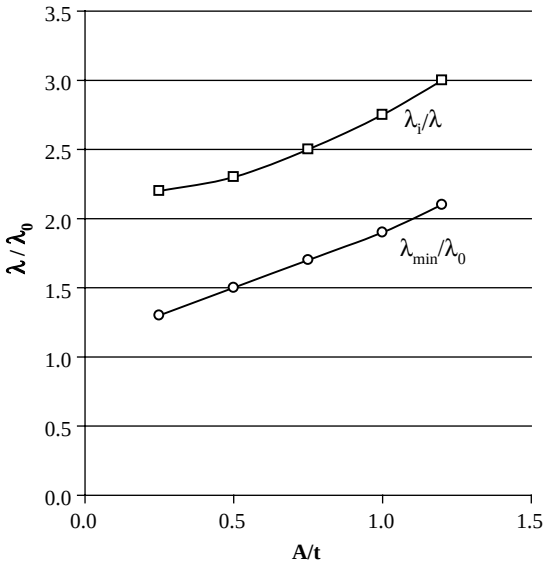

Fig. 14. Position of the intersection point for various $\zeta(\lambda_i/l_0)$ and the minimum for the buckling resistance ($\lambda_{\min}/l_0$).

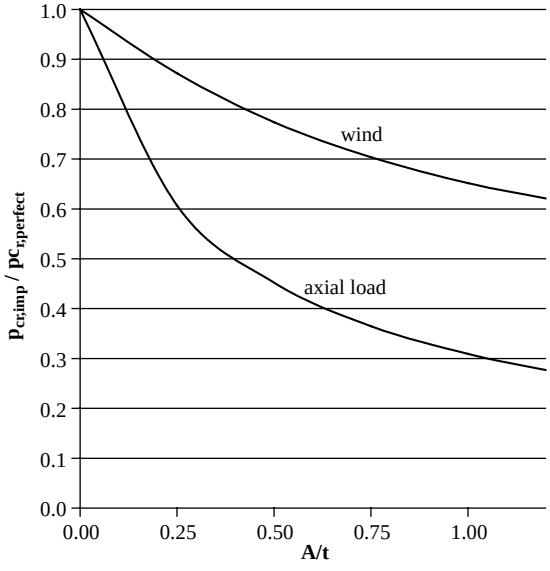

Fig. 15. Influence of imperfection amplitude on the buckling resistance.

buckling resistance levels out at a value equal to the value for a full circumferential weld. A similar behaviour was observed for other imperfection amplitudes. Consequently, it can be stated that a weld imperfection which spans only over 20° of the circumference must be viewed as equally detrimental as a full circumferential weld imperfection for cylinders under wind loading.

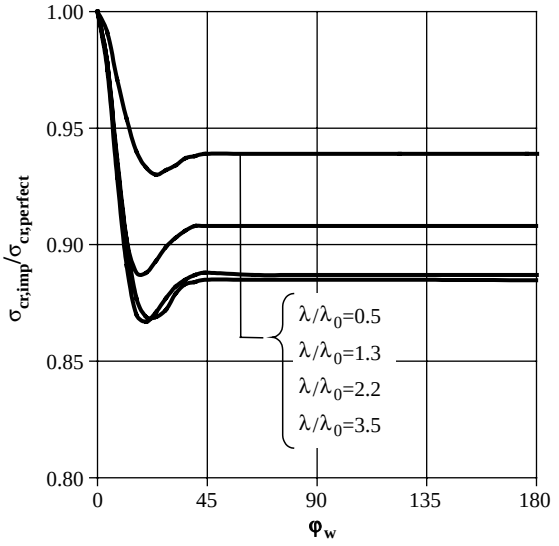

Fig. 16. Partial weld, amplitude $A/t = 0.25$.

3.5. Residual stresses

Shrinkage of the weld material not only introduces a geometrical imperfection into a cylindrical shell structure but also creates a residual stress field in the vicinity of the weld. Circumferential tension stresses at the weld often reach yield level and are typically balanced by significant compression stresses further away from the weld. The welding process creating this residual stress field can be approximated by applying appropriate strain loading at the weld. This method was first proposed by Rotter (1996) and was also used for this study. Comparing geometrically equal models with and without residual stress field showed that in the case of wind loading the buckling resistance was reduced due to residual stresses. However, for all considered cases this reduction was less than 2%.

3.6. Comparison with axial compression

The buckling behaviour of thin-walled cylinders with a weld imperfection in axial compression has been researched extensively. A comparison with the findings described in this paper for the wind loading case will be given in the following. Eq. (4) gives the classical buckling strength σ_{cl} of thin-walled cylinders in axial compression which will be used as a reference value for axial compression:

$$\sigma_{cl} = \frac{Et}{R\sqrt{3(1-\nu^2)}} \approx 0.605\frac{Et}{R}. \tag{4}$$

Teng and Rotter (1992) used a simplified shape function related to Eq. (2) in this paper and showed that the buckling resistance varied for $\zeta = 0.0$ and 1.0 for the same imperfection amplitude. Pircher and Bridge (2001) varied all three shape parameters (A/t, λ/λ_0 and ζ) of the shape function for imperfect cylinders and determined the influence of the weld shape on the buckling behaviour. Qualitatively this influence is very similar for both loading cases. The diagrams for axial compression given in Pircher and Bridge (2001) very much resemble the diagrams given in this paper in Figs. 9–13. For both loading cases the weld imperfection has been shown to lead to severe reductions in buckling resistance—significantly surpassing the influence of

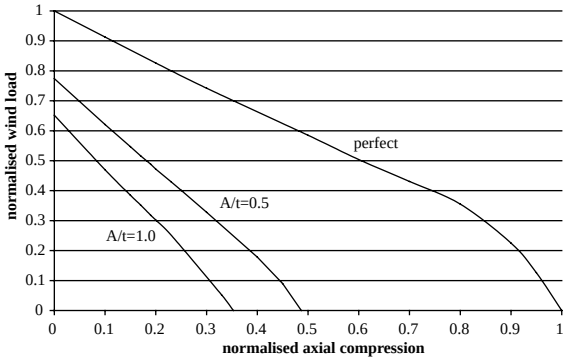

Fig. 17. Interaction diagram—axial compression and wind loading.

other imperfection shapes. The reduction of buckling resistance for various imperfection amplitudes for both loading cases can be seen in Fig. 15, where $p_{cr,perfect}$ refers to σ_{cl} as given in Eq. (4) for the axial loading case. While the position of the weld matters under wind loading, this is not the case for cylinders under axial compression (as long as the weld is positioned far enough away from the end constraints). Berry (1997) briefly investigated the effect of partial welds on the buckling behaviour under axial loading and found a similar behaviour as described in this paper for the wind loading case. Weld-induced residual stresses increase the buckling strength of cylindrical shell structures under axial loading by a small amount (Rotter, 1996; Pircher and Bridge, 2001) but decrease the buckling resistance of these structures under wind loading, again by a very small amount.

3.7. Interaction between wind loading and axial compression

Since axial compression and wind loading often occur simultaneously the interaction between the two loading cases was investigated. For the present study axial compression was applied onto the cylinder in a first step and wind loading was then applied and increased incrementally until stability failure occurred. Axial loading will be given normalised against σ_{cl}. Fig. 17 shows the interaction diagram for buckling under a combination of the two loading conditions for three different imperfection amplitudes ($A/t = 0.0,\ 0.5$ and 1.0). For the nominally perfect models the interaction diagram is slightly non-linear for cases with a high level of axial compression. For cylinders with weld imperfections the relationship is very close to linear.

4. Conclusions

A case study for a thin-walled cylindrical shell structure under wind loading has been presented. The geometric parameters of the cylinder were chosen so that a particular buckling pattern occurred. This pattern is characterised by horizontal ripple-like buckles in the upper half of the side of the cylinder facing the wind. In this area considerable axial compression occurs. Two critical factors trigger this type of stability failure: first, the ovalisation at the critical cross-section and secondly the disproportional increase of axial compression due to geometrically non-linear effects. Axi-symmetric weld imperfections were shown to reduce the buckling resistance of such a thin-walled cylinder considerably. An investigation into the nature of this influence has yielded the following results:

- The position of the weld along the height of the thin-walled cylinder has a great influence on the buckling strength under wind-loading. A weld positioned at 0.64 times the height of the cylinder leads to the greatest reduction in buckling strength.
- The shape of the weld imperfection can be described by three parameters: the ''roundness'', the half-wavelength and the amplitude. All three parameters influence the extent of the reduction.
- A partial weld spanning only 20° of the circumference already has the same effect as a full 360° weld imperfection.
- Weld-induced residual stress fields reduce the buckling resistance by a small amount.
- Strong similarities exist with the influence of such an imperfection on the buckling behaviour under axial compression. Interaction diagrams are given for the two loading conditions revealing an interaction characteristic which is close to linear.

Acknowledgements

The author thank Prof. R. Greiner and Prof. W. Guggenberger from the Institut für Stahlbau, Holzbau und Flächentragwerke at the Graz University of Technology in Austria and Prof. R.Q. Bridge from the Centre for Construction Technology and Research, University of Western Sydney in Australia for their support and their input into the work leading to this paper.

References

Berry, P.A., 1997. Buckling under axial compression of cylindrical shells with circumferential weld shrinkage depressions. PhD thesis, University of Sydney.

Berry, P.A., Rotter, J.M., Bridge, R.Q., 2000. Compression tests on cylinders with circumferential weld depressions. ASCE Journal of Engineering Mechanics 126 (4), 405–413.

Esslinger, M., 1971. Stationäre Windbelastung offener und geschlossener kreiszylindrischer Silos. Der Stahlbau 12, 361–368 (in German).

Feder, G., 1975. Einige qualitative Bemerkungen zum Beulen von stehenden Behältern unter Windlast. In: Esslinger, M., Geier, B. (Eds.), Sonderheft der Deutschen Forschungs- und Versuchsanstalt für Luft- und Raumfahrt, Braunschweig (in German).

Greiner, R., 1983. Zur ingenieurmässigen Berechnung und Konstruktion zylindrischer Behälter aus Stahl unter allgemeiner Belastung. Wissenschaft und Praxis, Band 31, Fachhochschule Biberach, Germany (in German).

Greiner, R., Derler, P., 1995. Effect of imperfections on wind-loaded cylindrical shells. Thin-Walled Structures 23, 271–281.

Kwok, K.C.S., 1985. Wind loads on circular storage bins. In: Proceedings: Joint US–Australian Workshop on Loading, Analysis and Stability of Thin Shell Bins, Tanks and Silos, University of Sydney, pp 49–54.

Macdonald, P.A., Kwok, K.C.S., Holmes, J.D., 1988. Wind loads on circular storage bins, silos and tanks: I. Point pressure measurements on isolated structures. Journal of Wind Engineering and Industrial Aerodynamics 31 (2–3), 165–188.

Pircher, M., 2004. Medium-length thin-walled cylinder under wind loading—a case study. Journal of Structural Engineering, ASCE (submitted for publication).

Pircher, M., Berry, P.A., Bridge, R.Q., 2000. The properties of circumferential weld-induced imperfections in silos and tanks. Engineering Report CE17, School of Engineering & Industrial Design, University of Western Sydney.

Pircher, M., Bridge, R.Q., 2001. Buckling of thin-walled silos and tanks under axial load some new aspects. Journal of Structural Engineering, ASCE 127 (10), 1129–1136.

Pircher, M., Berry, P.A., Ding, X., Bridge, R.Q., 2001a. The shape of circumferential weld-induced imperfections in thin-walled steel silos and tanks. Thin-Walled Structures 39 (12), 999–1014.

Pircher, M., Guggenberger, W., Greiner, R., 2001b. Stresses in elastically supported cylindrical shells under wind load and foundation settlement. Advances in Structural Engineering 4 (3), 159–167.

Rotter, J.M., Teng, J.G., 1989. Elastic stability of cylindrical shells with weld depressions. Journal of Structural Engineering, ASCE 115 (5), 1244–1263.

Rotter, J.M., 1996. Buckling and collapse in internally pressurised axially compressed silo cylinders with measured axisymmetric imperfections: imperfections, residual stresses and local collapse. In: Imperfections in Metal Silos Workshop, Lyon, France, pp 119–139.

Schneider, W., Zahlten, W., 2004. Load-bearing behaviour and structural analysis of slender ring-stiffened cylindrical shells under quasi-static wind load. Journal of Constructional Steel Research 60, 125–146.

Song, C.Y., Teng, J.G., Rotter, J.M., 2004. Imperfection sensitivity of thin elastic cylindrical shells subject to partial axial compression. International Journal of Solids and Structures (in press).

Steinhardt, O., Schulz, U., 1970. Zur Beulstabilität von Kreiszylinderschalen. Bericht der Versuchsanstalt fuer Stahl, Holz, Steine, Universitaet Karlsruhe (in German).

Teng, J.G., Rotter, J.M., 1992. Buckling of pressurised axisymmetrically imperfect cylinders under axial loads. Journal of Engineering Mechanics, ASCE 118 (2), 229–247.